Probing the three-gluon correlation functions by the single spin asymmetry in $p^\uparrow p \to DX$

YUJI KOIKE[1] AND SHINSUKE YOSHIDA[2]

[1] *Department of Physics, Niigata University, Ikarashi, Niigata 950-2181, Japan*
[2] *Graduate School of Science and Technology, Niigata University, Ikarashi, Niigata 950-2181, Japan*

Abstract

We study the single transverse-spin asymmetry for the inclusive open-charm production in the *pp*-collision, $p^\uparrow p \to DX$, induced by the three-gluon correlation functions in the polarized nucleon. We derive the corresponding twist-3 cross section formula in the leading order with respect to the QCD coupling constant. As in the case of the semi-inclusive deep inelastic scattering, $ep^\uparrow \to eDX$, our result differs from the previous result in the literature. We also derive a "master formula" which expresses the twist-3 cross section in terms of the $gg \to c\bar{c}$ hard scattering cross section. We present a model calculation of the asymmetry at the RHIC energy, demonstrating the sensitivity of the asymmetry on the form of the three-gluon correlation functions.

1

1 Introduction

Open charm production in inclusive hard processes, such as semi-inclusive deep inelastic scattering (SIDIS), $ep \to eDX$, and the D-meson production in pp collision, $pp \to DX$, is an ideal tool to investigate the gluon distributions in the nucleon. Similarly the single spin asymmetry (SSA) in those processes plays a crucial role to reveal the multi-gluon correlations in the nucleon [1, 2, 3, 4, 5, 6]. When the transverse momentum of the final D-meson can be regarded as hard ($P_T \gg \Lambda_{QCD}$), one can analyze the processes in the framework of the collinear factorization [7, 8, 9]. In this framework, SSA appears as a twist-3 observable and can be represented in terms of the multi-parton correlation functions. The purely gluonic correlations responsible for SSAs in the open charm production are represented by the "three-gluon" correlation functions. [1] For the quark-gluon correlation functions in the nucleon, there have been many studies in the literature in connection with SSAs for the light hadron productions [7]-[23], and our understanding on the mechanism of SSA has made a great progress.

In our recent paper [4] we studied the contribution from the three-gluon correlation functions to SIDIS, $ep^\uparrow \to eDX$. In that study, we have identified the complete set of the three-gluon correlation functions and established the formalism for calculating the twist-3 single-spin-dependent cross section induced by those functions. The gauge invariance and the factorization property of the cross section have been shown explicitly in the leading order with respect to the QCD coupling constant. The result of that study differs from the previous study in the literature [2], and we clarified the origin of the discrepancy. In our another paper [6], we have developed a novel "master formula" for the three-gluon contribution to $ep^\uparrow \to eDX$ which expresses the corresponding twist-3 cross section in terms of the twist-2 $\gamma^* g \to c\bar{c}$ scattering cross section, extending the similar formula known for the soft-gluon-pole (SGP) contribution to SSA from the quark-gluon correlation functions in the nucleon [16, 17]. This formula simplifies the actual calculation of the twist-3 cross section and makes its structure transparent, and may be useful to include higher order corrections to the asymmetry.

The purpose of this paper is to extend these studies to the contribution of the three-gluon correlation functions to the SSA in the pp collision,

$$p^\uparrow(p, S_\perp) + p(p') \to D(P_h) + X, \tag{1}$$

where $S_\perp$ is the transverse spin vector of the polarized nucleon and P_h is the momentum of the D-meson satisfying $P_h^2 = m_h^2$ with the D-meson mass m_h. The initial nucleons' momenta p and p' are in the collinear configuration and can be regarded as massless ($p^2 = p'^2 = 0$) in the twist-3 accuracy. We will derive a corresponding formula for the twist-3 single-spin-dependent cross section in the leading order with respect to the QCD coupling constant. We will further derive a master formula for (1) which connects the twist-3 cross section to the cross section for the $gg \to c\bar{c}$ scattering. We will also present a model calculation for

---

[1] In the framework of the transverse-momentum-dependent factorization, which is useful to describe the low-P_T hadron production, the corresponding gluonic effect is represented as the $k_\perp$-dependent gluon distribution functions [24, 25].

the asymmetry $A_N = \Delta\sigma/\sigma \equiv (\sigma^\uparrow - \sigma^\downarrow)/(\sigma^\uparrow + \sigma^\downarrow)$, where $\sigma^{\uparrow(\downarrow)}$ represents the cross section for (1) with the initial nucleon polarized along $S_\perp$ ($-S_\perp$), and will obtain a constraint on the three-gluon correlation functions, using the recent RHIC data on A_N for the D-meson production [26].

The remainder of this paper is organized as follows: In section 2, we recall the complete set of the three-gluon correlation functions in the transversely polarized nucleon which are relevant for our study. In section 3, we derive the twist-2 unpolarized cross section for the process $pp \to DX$ induced by the gluon-density in the nucleon. In section 4, we derive the twist-3 single-spin-dependent cross section induced by the three-gluon correlation functions for the process (1), applying the formalism in [4]. In section 5, we derive the master formula which expresses the twist-3 cross section for (1) induced by the three-gluon correlation functions in terms of the cross section for $gg \to c\bar{c}$ scattering in the twist-2 level. In section 6, we present a model calculation of A_N for the D-meson production at the RHIC energy, and demonstrate a sensitivity of the asymmetry on the form of the three-gluon correlation functions. Section 7 is devoted to a brief summary. In the appendix, we discuss some technical aspects in the derivation of the contribution from the initial-state-interaction diagrams to the twist-3 cross section.

2 Three-gluon correlation functions in the transversely polarized nucleon

The twist-3 three-gluon correlation functions in the transversely polarized nucleon were first introduced in [1]. Then, as was clarified in [27, 28, 4], there are two independent three-gluon correlation functions due to the difference in the contraction of color indices. Following the notation in [4], we call those functions $O(x_1, x_2)$ and $N(x_1, x_2)$, which are defined from the lightcone correlation functions of the three field-strengths of the gluon in the polarized nucleon as

$$O^{\alpha\beta\gamma}(x_1, x_2) = -g(i)^3 \int \frac{d\lambda}{2\pi} \int \frac{d\mu}{2\pi} e^{i\lambda x_1} e^{i\mu(x_2 - x_1)} \langle pS | d_{bca} F_b^{\beta n}(0) F_c^{\gamma n}(\mu n) F_a^{\alpha n}(\lambda n) | pS \rangle$$

$$= 2iM_N \left[O(x_1, x_2) g^{\alpha\beta} \epsilon^{\gamma pnS_\perp} + O(x_2, x_2 - x_1) g^{\beta\gamma} \epsilon^{\alpha pnS_\perp} + O(x_1, x_1 - x_2) g^{\gamma\alpha} \epsilon^{\beta pnS_\perp} \right], \quad (2)$$

$$N^{\alpha\beta\gamma}(x_1, x_2) = -g(i)^3 \int \frac{d\lambda}{2\pi} \int \frac{d\mu}{2\pi} e^{i\lambda x_1} e^{i\mu(x_2 - x_1)} \langle pS | i f_{bca} F_b^{\beta n}(0) F_c^{\gamma n}(\mu n) F_a^{\alpha n}(\lambda n) | pS \rangle$$

$$= 2iM_N \left[N(x_1, x_2) g^{\alpha\beta} \epsilon^{\gamma pnS_\perp} - N(x_2, x_2 - x_1) g^{\beta\gamma} \epsilon^{\alpha pnS_\perp} - N(x_1, x_1 - x_2) g^{\gamma\alpha} \epsilon^{\beta pnS_\perp} \right]. \quad (3)$$

where $F_a^{\alpha\beta} \equiv \partial^\alpha A_a^\beta - \partial^\beta A_a^\alpha + g f_{abc} A_b^\alpha A_c^\beta$ is the gluon's field strength, and we used the notation $F_a^{\alpha n} \equiv F_a^{\alpha\beta} n_\beta$ and $\epsilon^{\alpha pnS_\perp} \equiv \epsilon^{\alpha\mu\nu\lambda} p_\mu n_\nu S_{\perp\lambda}$ with the convention $\epsilon_{0123} = 1$. d^{bca} and f^{bca} are the symmetric and anti-symmetric structure constants of the color SU(3) group, and we have suppressed the gauge-link operators which ensure the gauge invariance. p is the nucleon momentum, and $S_\perp$ is the transverse spin vector of the nucleon normalized

as $S_\perp^2 = -1$. In the twist-3 accuracy, p can be regarded as lightlike ($p^2 = 0$), and n is another lightlike vector satisfying $p \cdot n = 1$. To be specific, we set $p^\mu = (p^+, 0, \mathbf{0}_\perp)$, $n^\mu = (0, n^-, \mathbf{0}_\perp)$, and $S_\perp^\mu = (0, 0, \mathbf{S}_\perp)$. The nucleon mass M_N is introduced to define $O(x_1, x_2)$ and $N(x_1, x_2)$ dimensionless. The decomposition (2) and (3) takes into account all the constraints from hermiticity, invariance under the parity- and time-reversal transformations and the permutation symmetry among the participating three gluon-fields. The functions $O(x_1, x_2)$ and $N(x_1, x_2)$ are real and have the following symmetry properties,

$$O(x_1, x_2) = O(x_2, x_1), \qquad O(x_1, x_2) = O(-x_1, -x_2), \tag{4}$$

$$N(x_1, x_2) = N(x_2, x_1), \qquad N(x_1, x_2) = -N(-x_1, -x_2). \tag{5}$$

3   Twist-2 unpolarized cross section for $pp \to DX$ from gluon-fusion

We first recall the twist-2 unpolarized cross section for the process (1) which is the denominator of A_N. It receives main contribution from the $c\bar{c}$-creation due to the gluon-fusion with the subsequent fragmentation of the c (or $\bar{c}$) quark into the D (or $\bar{D}$) meson (Fig. 1). The corresponding unpolarized cross section can be written as

$$P_h^0 \frac{d\sigma}{d^3 P_h} = \frac{\alpha_s^2}{S} \sum_{f=c,\bar{c}} \int \frac{dx'}{x'} G(x') \int \frac{dz}{z^2} D_f(z) \int \frac{dx}{x} G(x) \hat{\sigma}_{gg \to c}^U \delta(\tilde{s} + \tilde{t} + \tilde{u}) \tag{6}$$

where $S = (p + p')^2$ is the center-of-mass energy squared and $\alpha_s = g^2/(4\pi)$ is the strong coupling constant. The $c \to D$ (or $\bar{c} \to \bar{D}$) fragmentation function $D_f(z)$ and the unpolarized gluon distribution in the nucleon $G(x)$ are, respectively, defined as

$$\sum_X \frac{1}{N} \int \frac{d\lambda}{2\pi} e^{-i\lambda/z} \langle 0|\psi_i(0)|D(P_h)X\rangle \langle D(P_h)X|\bar{\psi}_j(\lambda w)|0\rangle = (\slashed{p}_c + m_c)_{ij} D_f(z) + \cdots, \tag{7}$$

$$\frac{1}{x} \int \frac{d\lambda}{2\pi} e^{i\lambda x} \langle p|F_a^{\mu n}(0) F_a^{\nu n}(\lambda n)|p\rangle = -\frac{1}{2} G(x) g_\perp^{\mu\nu} + \cdots, \tag{8}$$

where $N = 3$ is the number of colors, p_c is the momentum of the c (or $\bar{c}$) quark fragmenting into the D ($\bar{D}$)-meson with $p_c^2 = m_c^2$ and w is another lightlike vector of $O(1/p^+)$ satisfying $P_h \cdot w = 1$. Thus p_c is related to P_h as $p_c^\mu = P_h^\mu/z + (m_c^2 z - m_h^2/z)/2w^\mu$. $g_\perp^{\mu\nu}$ is defined as $g_\perp^{\mu\nu} \equiv g^{\mu\nu} - p^\mu n^\nu - p^\nu n^\mu$. The symbol $\cdots$ denotes higher-twist contributions which are irrelevant here. The partonic hard cross section $\hat{\sigma}_{gg \to c}^U$ can be obtained from the 9 diagrams shown in Fig. 2 in the leading order (LO) with respect to the QCD coupling constant, and is given by

$$\hat{\sigma}_{gg \to c}^U = \frac{1}{2N} \left(\frac{1}{\tilde{t}\tilde{u}} - \frac{N}{C_F} \frac{1}{\tilde{s}^2} \right) \left(\tilde{t}^2 + \tilde{u}^2 + 4m_c^2 \tilde{s} - \frac{4m_c^4 \tilde{s}^2}{\tilde{t}\tilde{u}} \right), \tag{9}$$
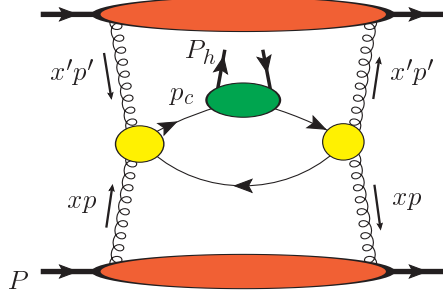
4

Figure 1: Generic diagrams for the twist-2 cross section for $pp \to DX$ induced by the gluon densities in the initial nucleons.
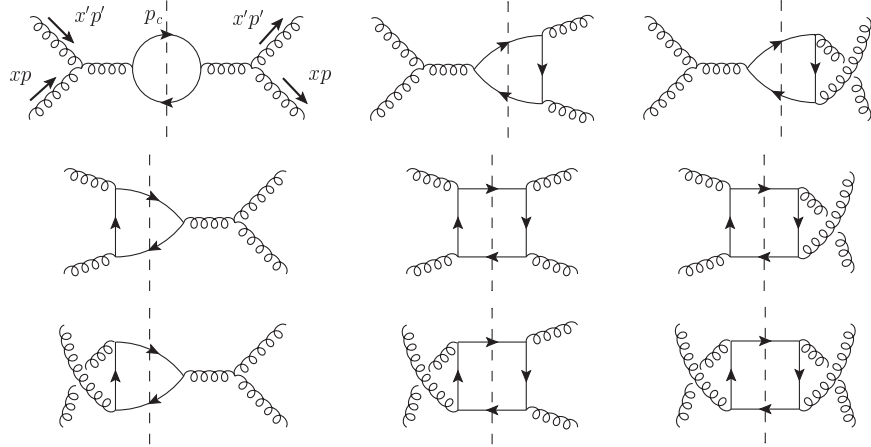

Figure 2: Leading order diagrams for the twist-2 unpolarized hard cross section for $\hat{\sigma}^U_{gg \to c}$ appearing in (6).

where the invariants for $gg \to c\bar{c}$ scattering are defined as

$$\tilde{s} = (xp + x'p')^2 \quad \tilde{t} = (p_c - xp)^2 - m_c^2 \quad \tilde{u} = (p_c - x'p')^2 - m_c^2, \tag{10}$$

and $C_F = \frac{N^2-1}{2N}$.

4   Twist-3 cross section for $p^\uparrow p \to DX$ induced by the three-gluon correlation functions

The twist-3 single-spin-dependent cross section for $p^\uparrow p \to DX$ induced by the three-gluon correlation functions can be obtained by applying the formalism developed for $ep^\uparrow \to eDX$ [4]. The twist-3 cross section occurs from the diagrams of the type shown in Fig.
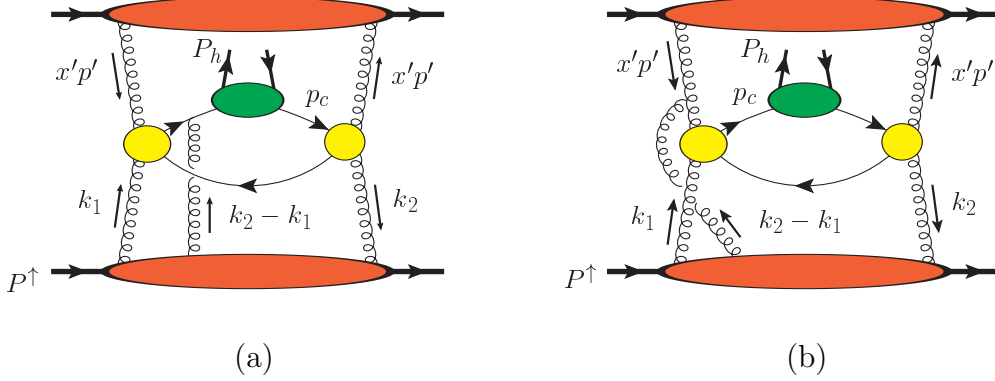
Figure 3: Generic diagrams which give the twist-3 cross section for $p^\uparrow p \to DX$ induced by the purely gluonic effect in the polarized nucleon (lower blob) convoluted with the unpolarized gluon density (upper blob) and the twist-2 fragmentation function for the D-meson (middle blob). A pair of circles in each figure represent $gg \to c\bar{c}$ hard scattering amplitudes. Figures (a) and (b) represent, respectively, the contributions from the final-state-interaction (FSI) and the initial-state-interaction (ISI). The mirror diagrams also contribute.

3, where the extra coherent gluon is exchanged between the hard scattering part and the nucleon matrix element. In Fig. 3, the gluon density $G(x')$ in the unpolarized cross section (upper blob) and the fragmentation function $D_f(z)$ for the D-meson (middle blob) are already factorized. Owing to the symmetry property of the correlation functions (lower blobs of Figs. 3(a) and (b)) defined by

$$M_{abc}^{\mu\nu\lambda}(k_1, k_2) = g \int d^4\xi \int d^4\eta\, e^{ik_1\xi} e^{i(k_2-k_1)\eta} \langle pS|A_b^\nu(0)A_c^\lambda(\eta)A_a^\mu(\xi)|pS\rangle, \qquad (11)$$

the SSA occurs only from a pole part of an internal propagator in the corresponding hard part

$$S_{\mu\nu\lambda}^{abc}(k_1, k_2, x'p', p_c), \qquad (12)$$

where a, b, c are color indices and the momenta k_1 and k_2 are assigned as shown in Fig. 3. Here and below we employ the convention that the QCD coupling constant g associated with the attachment of the coherent gluon into the hard part is included in the matrix element (11) consistently with the definition of the three-gluon correlation functions in (2) and (3). The hard part of the diagrams in Fig. 3 gives rise to the pole contributions at $x_1 = x_2$. (See discussions below.) For those contributions, following the same step as [4] in the collinear expansion to $S_{\mu\nu\lambda}^{abc}(k_1, k_2, x'p', p_c)$, we eventually end up with the following expression for the LO twist-3 cross section induced by the three-gluon correlation function (see Appendix):

$$P_h^0 \frac{d\Delta\sigma}{d^3P_h} = \frac{\alpha_s^2}{S} \sum_{f=c,\bar{c}} \int \frac{dx'}{x'} G(x') \int \frac{dz}{z^2} D_f(z) \int \frac{dx_1}{x_1} \int \frac{dx_2}{x_2}$$

$$\times \left[\frac{\partial S_{\mu\nu\lambda}^{abc}(k_1, k_2, x'p', p_c)p^\lambda}{\partial k_2^\sigma}\bigg|_{k_i = x_i p}\right]^{\text{pole}} \omega^\mu{}_\alpha \omega^\nu{}_\beta \omega^\sigma{}_\gamma M_{F,abc}^{\alpha\beta\gamma}(x_1, x_2), \quad (13)$$

where $\omega^\mu{}_\alpha = g^\mu{}_\alpha - p^\mu n_\alpha$, and $M_{F,abc}^{\alpha\beta\gamma}(x_1, x_2)$ is the lightcone correlation function of the field-strengths defined as

$$M_{F,abc}^{\alpha\beta\gamma}(x_1, x_2) = -g(i)^3 \int \frac{d\lambda}{2\pi} \int \frac{d\mu}{2\pi} e^{i\lambda x_1} e^{i\mu(x_2 - x_1)} \langle pS|F_b^{\beta n}(0)F_c^{\gamma n}(\mu n)F_a^{\alpha n}(\lambda n)|pS\rangle$$

$$= \frac{N d_{bca}}{(N^2 - 4)(N^2 - 1)} O^{\alpha\beta\gamma}(x_1, x_2) - \frac{i f_{bca}}{N(N^2 - 1)} N^{\alpha\beta\gamma}(x_1, x_2) \quad (14)$$

with $O^{\alpha\beta\gamma}(x_1, x_2)$ and $N^{\alpha\beta\gamma}(x_1, x_2)$ defined in (2) and (3), respectively. The symbol $[\cdots]^{\text{pole}}$ indicates the pole contribution is to be taken from the hard part. We emphasize that even though the analysis of Fig. 3 starts with the gauge-noninvariant correlation function (11) and the corresponding hard part $S_{\mu\nu\lambda}^{abc}(k_1, k_2, x'p', p_c)$, gauge-noninvariant contributions appearing in the collinear expansion either vanish or cancel and the total surviving twist-3 contribution to the single-spin-dependent cross section can be expressed as in (13), using the gauge-invariant correlation functions (2) and (3).
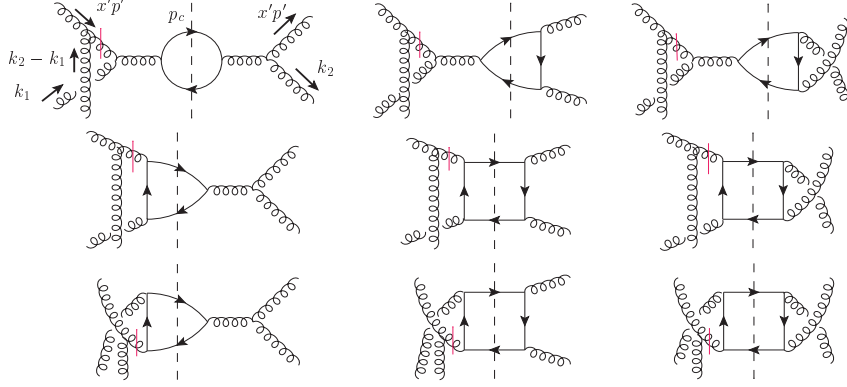
The pole contribution to the hard part $\left[\partial S_{\mu\nu\lambda}^{abc}(k_1, k_2, x'p', p_c)p^\lambda/\partial k_2^\sigma\big|_{k_i = x_i p}\right]^{\text{pole}}$ occurs from two types of diagrams shown in Figs. 3 (a) and 3(b), which are refered to as the final state interaction (FSI) and the initial state interaction (ISI), respectively, by the parton lines to which the coherent gluon is attached. Figs. 4 (a) and 4(b) show the LO diagrams contributing to the hard part $S_{\mu\nu\lambda}^{abc}(k_1, k_2, x'p', p_c)$ in Figs. 3(a) (FSI) and 3(b) (ISI), respectively. The mirror diagrams of Fig. 4 also contribute. The poles are produced from the bared propagator, and gives rise to the δ-function at $x_1 = x_2$ in the collinear limit $(k_i \to x_i p)$, hence the poles are refered to as the soft-gluon-pole (SGP). Other pole contributions cancel among each other by taking the sum of the whole diagrams.

By calculating $\left[\partial S_{\mu\nu\lambda}^{abc}(k_1, k_2, x'p', p_c)p^\lambda/\partial k_2^\sigma\big|_{k_i = x_i p}\right]^{\text{pole}}$ from Fig. 4 contracted with the coefficient tensors in the decomposition of (2) and (3), one obtains the twist-3 single-spin-dependent cross section as [5]

$$P_h^0 \frac{d\Delta\sigma}{d^3 P_h} = \frac{\alpha_s^2 M_N \pi}{S} \epsilon^{P_h p n S_\perp} \sum_{f = c\bar{c}} \int \frac{dx'}{x'} G(x') \int \frac{dz}{z^2} D_f(z) \int \frac{dx}{x} \delta\left(\tilde{s} + \tilde{t} + \tilde{u}\right) \frac{1}{z\tilde{u}}$$

$$\times \left[\delta_f \left\{\left(\frac{d}{dx}O(x,x) - \frac{2O(x,x)}{x}\right)\hat{\sigma}^{O1} + \left(\frac{d}{dx}O(x,0) - \frac{2O(x,0)}{x}\right)\hat{\sigma}^{O2} + \frac{O(x,x)}{x}\hat{\sigma}^{O3} + \frac{O(x,0)}{x}\hat{\sigma}^{O4}\right\}\right.$$

$$+ \left.\left\{\left(\frac{d}{dx}N(x,x) - \frac{2N(x,x)}{x}\right)\hat{\sigma}^{N1} + \left(\frac{d}{dx}N(x,0) - \frac{2N(x,0)}{x}\right)\hat{\sigma}^{N2} + \frac{N(x,x)}{x}\hat{\sigma}^{N3} + \frac{N(x,0)}{x}\hat{\sigma}^{N4}\right\}\right].$$

$$(15)$$
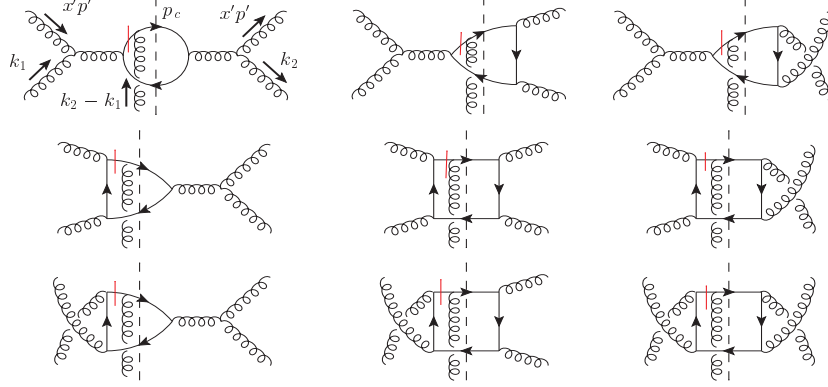
(a)

(b)

Figure 4: The LO diagrams for the partonic hard part $S^{abc}_{\mu\nu\lambda}(k_1, k_2, x'p', p_c)$ for the twist-3 cross section. Diagrams in (a) represent the FSI contribution and those in (b) represent the ISI contribution.

where $\delta_c = 1$ and $\delta_{\bar{c}} = -1$. The partonic hard cross sections are given by

$$
\begin{cases}
\hat{\sigma}^{O1} = \left(\dfrac{1}{C_F} \dfrac{\tilde{u} - \tilde{t}}{\tilde{s}\tilde{t}\tilde{u}} + \dfrac{1}{C_F} \dfrac{\tilde{u}}{\tilde{s}\tilde{t}^2} - \dfrac{1}{N^2 C_F} \dfrac{\tilde{s}}{\tilde{t}^2\tilde{u}} \right) \left(\tilde{t}^2 + \tilde{u}^2 + 4m_c^2\tilde{s} - \dfrac{4m_c^4\tilde{s}^2}{\tilde{t}\tilde{u}} \right), \\[4mm]
\hat{\sigma}^{O2} = \left(\dfrac{1}{C_F} \dfrac{\tilde{u} - \tilde{t}}{\tilde{s}\tilde{t}\tilde{u}} + \dfrac{1}{C_F} \dfrac{\tilde{u}}{\tilde{s}\tilde{t}^2} - \dfrac{1}{N^2 C_F} \dfrac{\tilde{s}}{\tilde{t}^2\tilde{u}} \right) \left(\tilde{t}^2 + \tilde{u}^2 + 8m_c^2\tilde{s} - \dfrac{8m_c^4\tilde{s}^2}{\tilde{t}\tilde{u}} \right), \\[4mm]
\hat{\sigma}^{O3} = \left(\dfrac{1}{C_F} \dfrac{\tilde{u} - \tilde{t}}{\tilde{t}^2\tilde{u}^2} + \dfrac{1}{C_F} \dfrac{1}{\tilde{t}^3} - \dfrac{1}{N^2 C_F} \dfrac{\tilde{s}^2}{\tilde{t}^3\tilde{u}^2} \right) \left(8m_c^4\tilde{s} - 4m_c^2\tilde{t}\tilde{u} \right), \\[4mm]
\hat{\sigma}^{O4} = \left(\dfrac{1}{C_F} \dfrac{\tilde{u} - \tilde{t}}{\tilde{t}^2\tilde{u}^2} + \dfrac{1}{C_F} \dfrac{1}{\tilde{t}^3} - \dfrac{1}{N^2 C_F} \dfrac{\tilde{s}^2}{\tilde{t}^3\tilde{u}^2} \right) \left(16m_c^4\tilde{s} - 4m_c^2\tilde{t}\tilde{u} \right),
\end{cases}
\tag{16}
$$

8

and

$$
\begin{cases}
\hat{\sigma}^{N1} = \left(\dfrac{1}{C_F} \dfrac{\tilde{t}^2 + \tilde{u}^2}{\tilde{s}^2 \tilde{t} \tilde{u}} + \dfrac{1}{C_F} \dfrac{\tilde{u}}{\tilde{s}\tilde{t}^2} - \dfrac{1}{N^2 C_F} \dfrac{\tilde{s}}{\tilde{t}^2 \tilde{u}} \right) \left(\tilde{t}^2 + \tilde{u}^2 + 4 m_c^2 \tilde{s} - \dfrac{4 m_c^4 \tilde{s}^2}{\tilde{t}\tilde{u}} \right), \\[14pt]
\hat{\sigma}^{N2} = -\left(\dfrac{1}{C_F} \dfrac{\tilde{t}^2 + \tilde{u}^2}{\tilde{s}^2 \tilde{t} \tilde{u}} + \dfrac{1}{C_F} \dfrac{\tilde{u}}{\tilde{s}\tilde{t}^2} - \dfrac{1}{N^2 C_F} \dfrac{\tilde{s}}{\tilde{t}^2 \tilde{u}} \right) \left(\tilde{t}^2 + \tilde{u}^2 + 8 m_c^2 \tilde{s} - \dfrac{8 m_c^4 \tilde{s}^2}{\tilde{t}\tilde{u}} \right), \\[14pt]
\hat{\sigma}^{N3} = \left(\dfrac{1}{C_F} \dfrac{\tilde{t}^2 + \tilde{u}^2}{\tilde{s}\tilde{t}^2 \tilde{u}^2} + \dfrac{1}{C_F} \dfrac{1}{\tilde{t}^3} - \dfrac{1}{N^2 C_F} \dfrac{\tilde{s}^2}{\tilde{t}^3 \tilde{u}^2} \right) \left(8 m_c^4 \tilde{s} - 4 m_c^2 \tilde{t} \tilde{u} \right), \\[14pt]
\hat{\sigma}^{N4} = -\left(\dfrac{1}{C_F} \dfrac{\tilde{t}^2 + \tilde{u}^2}{\tilde{s}\tilde{t}^2 \tilde{u}^2} + \dfrac{1}{C_F} \dfrac{1}{\tilde{t}^3} - \dfrac{1}{N^2 C_F} \dfrac{\tilde{s}^2}{\tilde{t}^3 \tilde{u}^2} \right) \left(16 m_c^4 \tilde{s} - 4 m_c^2 \tilde{t} \tilde{u} \right),
\end{cases}
\tag{17}
$$

The hard cross sections associated with the first term in the first parentheses in (16) and (17) come from ISI (Fig. 4(b)), and those associated with the second and the third terms in the same parentheses come from FSI (Fig. 4(a)). As in the case of $ep^\uparrow \to eDX$, the cross section in (15) receives the contribution from the four functions $O(x, x)$, $O(x, 0)$, $N(x, x)$ and $N(x, 0)$. Unlike the case of SIDIS, presence of ISI gives rise to the different hard cross sections for O and N functions. From (15), it is clear that the process $p^\uparrow p \to DX$ itself is not sufficient for the complete separation of the four functions. For the separation, the process $ep^\uparrow \to eDX$ serves greatly, since it has five structure functions with different dependences on the azimuthal angles to which the four functions contribute differently [4]. For the massless quark fragmenting into a light hadron (i.e. $m_c \to 0$), one has $\hat{\sigma}^{O3, O4, N3, N4} \to 0$, $\sigma^{O1} = \sigma^{O2}$ and $\sigma^{N1} = -\sigma^{N2}$. Therefore the three-gluon correlation functions appear in the combination of $x(d/dx)(O(x, x) + O(x, 0)) - 2(O(x, x) + O(x, 0))$ and $x(d/dx)(N(x, x) - N(x, 0)) - 2(N(x, x) - N(x, 0))$ at $m_c = 0$.

Our result in (15) differs from a previous work [3]: The result in [3] is obtained from (15) by omitting the terms with $\hat{\sigma}^{O2, O4}$ and $\hat{\sigma}^{N2, N4}$ and by the replacement $O(x, x) \to O(x, x) + O(x, 0)$ and $N(x, x) \to N(x, x) - N(x, 0)$. This difference originates from an ad-hoc assumption in the factorization formula in [3, 2]. We emphasize the appearance of the four different contributions with $\{O(x, x), O(x, 0), N(x, x), N(x, 0)\}$ is a consequence of the symmetry property implied in the decomposition (2) and (3), in particular, the different coefficient tensors in front of $O(x, x)$ and $O(x, 0)$ (likewise for $N(x, x)$ and $N(x, 0)$) at $x_1 = x_2 = x$ lead to different hard cross sections for the above four functions. See [4] for more details.

5 Master formula for the three-gluon contribution to $p^\uparrow p \to DX$

5.1 Connection between the twist-3 cross section and the $gg \to c\bar{c}$ scattering

To obtain the twist-3 cross section based on (13), one has to calculate the derivative of the hard part $[\partial S_{\mu\nu\lambda}^{abc}(k_1, k_2, x'p', p_c) p^\lambda / \partial k_2^\sigma \big|_{k_i = x_i p}]^{\text{pole}}$ from Fig. 4 contracted with the coefficient

9

tensors in the decomposition of (2) and (3). This calculation produces lots of terms at the intermediate step and is extremely complicated. Alternatively, application of the "master formula" developed for the contribution of the quark-gluon correlation functions [16, 17] and also for the three-gluon correlations for $ep^\uparrow \to eDX$ [6] provides us with a more transparent and simpler method to calculate the cross section. To extend the method to the contribution of the three-gluon correlation functions for $p^\uparrow p \to DX$, we first note that the diagrams in Fig. 4 are obtained by attaching the extra gluon-line to the external-lines of the twist-2 hard part in Fig. 2, and the pole contribution is given by the propagator next to the vertex to which this extra-gluon line attaches. Because of this structure, the derivative can be performed by keeping the structure of the hard part corresponding to those in Fig. 2 almost intact. Based on this observation, one can obtain the master formula also for the three-gluon contribution. To be specific, we consider the case in which the c-quark fragments into the D-meson below.

To present the result, we first define the hard part for the unpolarized cross section shown in Fig. 2 as $\mathcal{H}_{\mu\nu}^{U,ab}(xp, x'p', p_c)$, where $\mu\nu$ and ab are, respectively, the Lorentz and the color indices for the gluon line with the momentum xp. Those indices for the gluon line with the momentum $x'p'$ are already contracted to factorize $G(x')$ in (6). With this convention the partonic hard cross section $\hat{\sigma}_{gg\to c}$ in (6) is related to $\mathcal{H}_{\mu\nu}^{U,ab}$ as

$$\hat{\sigma}_{gg\to c}^{U}(\tilde{s}, \tilde{t}, \tilde{u}, m_c^2)\delta\left(\tilde{s} + \tilde{t} + \tilde{u}\right) = \frac{1}{(N^2-1)}\delta_{ab}\left(-\frac{1}{2}g_\perp^{\mu\nu}\right)\mathcal{H}_{\mu\nu}^{U,ab}(xp, x'p', p_c). \qquad (18)$$

As is shown below the hard part for the twist-3 cross section has a simple relation with this $\mathcal{H}_{\mu\nu}^{U,ab}(xp, x'p', p_c)$.

In [6], we have shown that the twist-3 hard cross section for $ep^\uparrow \to eDX$ induced by the three-gluon correlation functions can be obtained from the Born cross section for the $\gamma^* g \to c\bar{c}$ scattering. There the SGP contribution occurs from the FSI. Accordingly, the FSI contribution for $p^\uparrow p \to DX$ shown in Fig. 4(a) can also be expressed in terms of the Born cross section for the $gg \to c\bar{c}$ scattering. We write the FSI contribution to $S_{\mu\nu\lambda}^{abc}(k_1, k_2, x'p', p_c)p^\lambda$ in (13) as $S_{\mu\nu\lambda}^{F,abc}(k_1, k_2, x'p', p_c)p^\lambda$. Then, following the same procedure as [6], one can show that the hard part for the FSI is given by

$$\left[\frac{\partial S_{\mu\nu\lambda}^{F,abc}(k_1, k_2, x'p', p_c)p^\lambda}{\partial k_2^\sigma}\bigg|_{k_i=x_ip}\right]^{\text{pole}}$$

$$= \left[\frac{1}{x_1 - x_2 + i\epsilon}\right]^{\text{pole}}\left(\frac{\partial}{\partial p_c^\sigma} - \frac{p_{c\sigma}p^\lambda}{p\cdot p_c}\frac{\partial}{\partial p_c^\lambda}\right)\mathcal{H}_{\mu\nu}^{F,abc}(x_1p, x'p', p_c)$$

$$= \left[\frac{1}{x_1 - x_2 + i\epsilon}\right]^{\text{pole}}\frac{d}{dp_c^\sigma}\mathcal{H}_{\mu\nu}^{F,abc}(x_1p, x'p', p_c), \qquad (19)$$

where $\mathcal{H}_{\mu\nu}^{F,abc}(x_1p, x'p', p_c)$ is obtained from $\mathcal{H}_{\mu\nu}^{U,ab}(x_1p, x'p', p_c)$ simply by adding the extra color matrix t^c in the same place where the coherent gluon line is attached in Fig. 4(a).

10

Here one needs to be cautious in taking derivative with respect to p_c^σ: In the expression after the first equality of (19), the on-shell limit $p_c^2 = m_c^2$ should be taken after performing the derivative with respect to p_c^σ. For the derivative in the expression after the second equality of (19), the form $p_c^\mu = \left(p_c^+ = \frac{m_c^2 + \vec{p}_{c\perp}^2}{2p^-}, p_c^-, \vec{p}_{c\perp}\right)$ should be used for p_c, i.e., on-shell condition for p_c should be used by regarding p_c^+ as a dependent variable of p_c^- and $\vec{p}_{c\perp}$.

One can also derive the similar relation for the ISI contribution. We write the ISI contribution to $S_{\mu\nu\lambda}^{abc}(k_1, k_2, x'p', p_c)p^\lambda$ in (13) as $S_{\mu\nu\lambda}^{I,abc}(k_1, k_2, x'p', p_c)p^\lambda$. For the ISI diagrams in Fig. 4(b), the coherent gluon couples to the initial gluon-line of the diagrams in Fig. 2 through the three-gluon coupling. One can still apply the same method as [6], and obtains for the ISI contribution as

$$
\left[\left.\frac{\partial S_{\mu\nu\lambda}^{I,abc}(k_1, k_2, x'p', p_c)p^\lambda}{\partial k_2^\sigma}\right|_{k_i = x_i p}\right]^{\text{pole}}
$$

$$
= \left[\frac{-1}{x_2 - x_1 + i\epsilon}\right]^{\text{pole}} \left(\frac{\partial}{\partial(x'p'^\sigma)} - \frac{p'_\sigma p^\lambda}{p \cdot p'}\frac{\partial}{\partial(x'p'^\lambda)}\right) \mathcal{H}_{\mu\nu}^{I,abc}(x_1 p, x'p', p_c),
$$

$$
= \left[\frac{-1}{x_2 - x_1 + i\epsilon}\right]^{\text{pole}} \frac{d}{d(x'p'^\sigma)}\mathcal{H}_{\mu\nu}^{I,abc}(x_1 p, x'p', p_c), \tag{20}
$$

where $\mathcal{H}_{\mu\nu}^{I,abc}(x_1 p, x'p', p_c)$ differs from $\mathcal{H}_{\mu\nu}^{U,ab}(x_1 p, x'p', p_c)$ only with its extra color index c associated with the attachment of the coherent gluon line in Fig. 4(b). As in (19) the on-shell limit $p'^2 \to 0$ should be taken after carrying out the derivative in the expression after the first equality in (20), and the on-shell form $p'^\mu = \left(p'^+ = \frac{\vec{p'}_\perp^2}{2p'^-}, p'^-, \vec{p'}_\perp\right)$ should be used in the expression after the second equality of (20). In (20), we first make $p'^\sigma_\perp \neq 0$ in taking the derivative and then take the $p'^\sigma_\perp \to 0$ limit to consider the cross section in the frame where p and p' are collinear. Inserting (19) and (20) into (13), one obtains the single-spin-dependent cross section as

$$
P_h^0 \frac{d\Delta\sigma}{d^3 P_h} = \frac{\alpha_s^2}{S} \int \frac{dx'}{x'} G(x') \int \frac{dz}{z^2} D_c(z) \int \frac{dx}{x^2}(-i\pi)\omega^\mu{}_\alpha \omega^\nu{}_\beta \omega^\sigma{}_\gamma M_{F,abc}^{\alpha\beta\gamma}(x, x)
$$

$$
\times \left[\frac{d}{dp_c^\sigma}\mathcal{H}_{\mu\nu}^{F,abc}(xp, x'p', p_c) - \frac{d}{d(x'p'^\sigma)}\mathcal{H}_{\mu\nu}^{I,abc}(xp, x'p', p_c)\right]. \tag{21}
$$

The hard part $\mathcal{H}_{\mu\nu}^{F,abc}$ and $\mathcal{H}_{\mu\nu}^{I,abc}$ contain the factor $\delta\left((xp + x'p' - p_c)^2 - m_c^2\right) = \delta\left(\tilde{s} + \tilde{t} + \tilde{u}\right)$ as an on-shell condition for the final unobserved $\bar{c}$-quark. For convenience we separate this δ-function and introduce the following functions by taking the color contraction:

$$
\frac{N d_{bca}}{(N^2 - 1)(N^2 - 4)}\mathcal{H}_{\alpha\beta}^{F,abc}(xp, x'p', p_c) \equiv H_{\alpha\beta}^{(F,d)}(xp, x'p', p_c)\delta\left(\tilde{s} + \tilde{t} + \tilde{u}\right),
$$

$$
\frac{-i f_{bca}}{N(N^2 - 1)}\mathcal{H}_{\alpha\beta}^{F,abc}(xp, x'p', p_c) \equiv H_{\alpha\beta}^{(F,f)}(xp, x'p', p_c)\delta\left(\tilde{s} + \tilde{t} + \tilde{u}\right),
$$

11

$$\frac{Nd_{bca}}{(N^2-1)(N^2-4)}\mathcal{H}_{\alpha\beta}^{I,abc}(xp,x'p',p_c) \equiv H_{\alpha\beta}^{(I,d)}(xp,x'p',p_c)\delta\left(\tilde{s}+\tilde{t}+\tilde{u}\right),$$

$$\frac{-if_{bca}}{N(N^2-1)}\mathcal{H}_{\alpha\beta}^{I,abc}(xp,x'p',p_c) \equiv H_{\alpha\beta}^{(I,f)}(xp,x'p',p_c)\delta\left(\tilde{s}+\tilde{t}+\tilde{u}\right). \tag{22}$$

Using these forms in (21), one can write the cross section as

$$P_h^0\frac{d\Delta\sigma}{d^3P_h} = \frac{\alpha_s^2}{S}\int\frac{dx'}{x'}G(x')\int\frac{dz}{z^2}D_c(z)\int\frac{dx}{x^2}(-i\pi)$$

$$\times\left[O_\perp^{\alpha\beta\gamma}(x,x)\left\{\frac{d}{dp_c^\gamma}H_{\alpha\beta}^{(F,d)}(xp,x'p',p_c) - \frac{d}{d(x'p'^\gamma)}H_{\alpha\beta}^{(I,d)}(xp,x'p',p_c)\right\}\delta\left(\tilde{s}+\tilde{t}+\tilde{u}\right)\right.$$

$$\left.+N_\perp^{\alpha\beta\gamma}(x,x)\left\{\frac{d}{dp_c^\gamma}H_{\alpha\beta}^{(F,f)}(xp,x'p',p_c) - \frac{d}{d(x'p'^\gamma)}H_{\alpha\beta}^{(I,f)}(xp,x'p',p_c)\right\}\delta\left(\tilde{s}+\tilde{t}+\tilde{u}\right)\right],\tag{23}$$

where $O_\perp^{\alpha\beta\gamma}(x,x)$ and $N_\perp^{\alpha\beta\gamma}(x,x)$ are the functions obtained by setting $x_1=x_2=x$ in (2) and (3):

$$O_\perp^{\alpha\beta\gamma}(x,x) = 2iM_N\left[O(x,x)g_\perp^{\alpha\beta}\epsilon^{\gamma pnS_\perp} + O(x,0)(g_\perp^{\beta\gamma}\epsilon^{\alpha pnS_\perp} + g_\perp^{\gamma\alpha}\epsilon^{\beta pnS_\perp})\right],$$

$$N_\perp^{\alpha\beta\gamma}(x,x) = 2iM_N\left[N(x,x)g_\perp^{\alpha\beta}\epsilon^{\gamma pnS_\perp} - N(x,0)(g_\perp^{\beta\gamma}\epsilon^{\alpha pnS_\perp} + g_\perp^{\gamma\alpha}\epsilon^{\beta pnS_\perp})\right].\tag{24}$$

We remind the derivatives d/dp_c^γ and $d/d(x'p'^\gamma)$ in (23) also hit $\delta\left(\tilde{s}+\tilde{t}+\tilde{u}\right)$. The relation (23) shows that the partonic hard cross section for $O(x,x)$ and $O(x,0)$, in general, differ from each other, and likewise for $N(x,x)$ and $N(x,0)$.

5.2 Contribution from $O(x,x)$ and $N(x,x)$

We first consider the contribution in (23) occuring from $O(x,x)$ and $N(x,x)$ in (24). Using the functions (22), we write the corresponding hard part as

$$H_{\alpha\beta}^{(F,j)}(xp,x'p',p_c)g_\perp^{\alpha\beta}\epsilon^{\gamma pnS_\perp} \equiv K^{(F,j)}(\tilde{s},\tilde{t},\tilde{u},m_c^2)\epsilon^{\gamma pnS_\perp},$$

$$H_{\alpha\beta}^{(I,j)}(xp,x'p',p_c)g_\perp^{\alpha\beta}\epsilon^{\gamma pnS_\perp} \equiv K^{(I,j)}(\tilde{s},\tilde{t},\tilde{u},m_c^2)\epsilon^{\gamma pnS_\perp},\tag{25}$$

for $j=d,f$, where we have used the fact that the scalar functions $K^{(F,j)}$ and $K^{(I,j)}$ ($j=d,f$) become the functions of $\tilde{s}$, $\tilde{t}$, $\tilde{u}$ and m_c^2. For the scalar functions $K^{(F,j)}$, $K^{(I,j)}$ and $\delta\left(\tilde{s}+\tilde{t}+\tilde{u}\right)$, one can perform the derivative with respect to p_c^γ and $x'p'^\gamma$ in (23) through that with respect to $\tilde{u}$ as

$$\frac{d}{dp_c^\gamma}K^{(F,j)}(\tilde{s},\tilde{t},\tilde{u},m_c^2)\delta\left(\tilde{s}+\tilde{t}+\tilde{u}\right) = -2p_{c\gamma}\left(\frac{\tilde{s}}{\tilde{t}}\right)\frac{\partial}{\partial\tilde{u}}K^{(F,j)}(\tilde{s},\tilde{t},\tilde{u},m_c^2)\delta\left(\tilde{s}+\tilde{t}+\tilde{u}\right),\tag{26}$$

$$\frac{d}{d(x'p'^\gamma)}K^{(I,j)}(\tilde{s},\tilde{t},\tilde{u},m_c^2)\delta\left(\tilde{s}+\tilde{t}+\tilde{u}\right) = -2p_{c\gamma}\frac{\partial}{\partial\tilde{u}}K^{(I,j)}(\tilde{s},\tilde{t},\tilde{u},m_c^2)\delta\left(\tilde{s}+\tilde{t}+\tilde{u}\right),\tag{27}$$

12

for $j = d, f$, where we have used the fact that p_c^+ and p'^+ are the dependent variables (as noted after (19) and (20)), and have set $p'^\gamma_\perp \to 0$ after taking the derivative.[2] Using (26), one obtains for the FSI contribution with $O(x,x)$ in (23) as

$$\int \frac{dx}{x^2} O(x,x) \, \frac{d}{dp_c^\gamma} H_{\alpha\beta}^{(F,d)}(\tilde{s}, \tilde{t}, \tilde{u}, m_c^2) \delta\left(\tilde{s} + \tilde{t} + \tilde{u}\right) g_\perp^{\alpha\beta} \epsilon^{\gamma p n S_\perp}$$

$$= -2\epsilon^{p_c p n S_\perp} \int \frac{dx}{x^2} O(x,x) \left(\frac{\tilde{s}}{\tilde{t}}\right) \frac{\partial}{\partial \tilde{u}} K^{(F,d)}(\tilde{s}, \tilde{t}, \tilde{u}, m_c^2) \delta\left(\tilde{s} + \tilde{t} + \tilde{u}\right)$$

$$= -2\epsilon^{p_c p n S_\perp} \int \frac{dx}{x^2} \left(\frac{\tilde{s}}{\tilde{t}}\right) \left[\left(\frac{\partial K^{(F,d)}}{\partial \tilde{u}} + \frac{x}{\tilde{u}} \frac{\partial K^{(F,d)}}{\partial x} - \frac{2 K^{(F,d)}}{\tilde{u}}\right) O(x,x) + \frac{K^{(F,d)}}{\tilde{u}} x \frac{dO(x,x)}{dx}\right]$$

$$\times \delta\left(\tilde{s} + \tilde{t} + \tilde{u}\right)$$

$$= -2\epsilon^{p_c p n S_\perp} \int \frac{dx}{x^2} \left(\frac{\tilde{s}}{\tilde{t}}\right) \left[\left(\frac{\partial K^{(F,d)}}{\partial \tilde{u}} + \frac{\tilde{t}}{\tilde{u}} \frac{\partial K^{(F,d)}}{\partial \tilde{t}} + \frac{\tilde{s}}{\tilde{u}} \frac{\partial K^{(F,d)}}{\partial \tilde{s}} - \frac{2 K^{(F,d)}}{\tilde{u}}\right) O(x,x)\right.$$

$$\left. + \frac{K^{(F,d)}}{\tilde{u}} x \frac{dO(x,x)}{dx}\right] \delta\left(\tilde{s} + \tilde{t} + \tilde{u}\right)$$

$$= -2\epsilon^{p_c p n S_\perp} \int \frac{dx}{x^2} \left(\frac{\tilde{s}}{\tilde{t}\tilde{u}}\right) \left[-m_c^2 \frac{\partial K^{(F,d)}}{\partial m_c^2} O(x,x) + K^{(F,d)} \left(x \frac{dO(x,x)}{dx} - 2 O(x,x)\right)\right]$$

$$\times \delta\left(\tilde{s} + \tilde{t} + \tilde{u}\right). \tag{28}$$

In the first equality of (28), we transformed the derivative hitting $\delta\left(\tilde{s} + \tilde{t} + \tilde{u}\right)$ into the derivative with respect to x and performed the partial integration. In the last equality we have used the relation

$$\left(\tilde{s}\frac{\partial}{\partial \tilde{s}} + \tilde{t}\frac{\partial}{\partial \tilde{t}} + \tilde{u}\frac{\partial}{\partial \tilde{u}} + m_c^2\frac{\partial}{\partial m_c^2}\right) K^{(B,j)}(\tilde{s}, \tilde{t}, \tilde{u}, m_c^2) = 0, \tag{29}$$

for $B = F, I$ and $j = d, f$, resulting from the scale-invariance property for the dimensionless function $K^{(B,j)}(\tilde{s}, \tilde{t}, \tilde{u}, m_c^2) = K^{(B,j)}(\lambda\tilde{s}, \lambda\tilde{t}, \lambda\tilde{u}, \lambda m_c^2)$. Similarly to (28), by using (27), one obtains for the ISI contribution with $O(x,x)$ in (23) as

$$-\int \frac{dx}{x^2} O(x,x) \, \frac{d}{d(x'p'^\gamma)} H_{\alpha\beta}^{(I,d)}(\tilde{s}, \tilde{t}, \tilde{u}, m_c^2) \delta\left(\tilde{s} + \tilde{t} + \tilde{u}\right) g_\perp^{\alpha\beta} \epsilon^{\gamma p n S_\perp}$$

$$= 2\epsilon^{p_c p n S_\perp} \int \frac{dx}{x^2} O(x,x) \frac{\partial}{\partial \tilde{u}} K^{(I,d)}(\tilde{s}, \tilde{t}, \tilde{u}, m_c^2) \delta\left(\tilde{s} + \tilde{t} + \tilde{u}\right)$$

---

[2]For the FSI, one can set $p'^\gamma_\perp = 0$ from the beginning.

$$= 2\epsilon^{p_c p n S_\perp} \int \frac{dx}{x^2} \frac{1}{\tilde{u}} \left[-m_c^2 \frac{\partial K^{(I,d)}}{\partial m_c^2} O(x,x) + K^{(I,d)} \left(x \frac{dO(x,x)}{dx} - 2O(x,x) \right) \right] \delta \left(\tilde{s} + \tilde{t} + \tilde{u} \right).$$

(30)

By the replacement $K^{(B,d)}(\tilde{s}, \tilde{t}, \tilde{u}, m_c^2) \to K^{(B,f)}(\tilde{s}, \tilde{t}, \tilde{u}, m_c^2)$ $(B = F, I)$ and $O(x,x) \to N(x,x)$ in (28) and (30), one obtains the formula for the $N(x,x)$ contributions. From (28) and (30), one can make the following important observations for the $O(x,x)$ and $N(x,x)$ contributions:

(1) The partonic hard cross sections for $x\frac{d}{dx}O(x,x)$ and $O(x,x)$ are connected by the simple relation. In particular, in the $m_c \to 0$ limit, they contribute in the form $x\frac{d}{dx}O(x,x) - 2O(x,x)$. The same relation holds for $x\frac{d}{dx}N(x,x)$ and $N(x,x)$.

(2) The partonic hard cross sections $K^{(B,j)}$ $(B = F, I,\ j = d, f)$ defined in (25) are obtained from $\mathcal{H}_{\mu\nu}^{F,abc}$ and $\mathcal{H}_{\mu\nu}^{I,abc}$ by the same Lorentz contraction as the unpolarized cross section in (18). Therefore the contribution to $K^{(B,j)}$ from each diagram differs from those for $\hat{\sigma}_{gg \to c}^U$ only in the color factors.

These features are the extension of those obtained in [17] for the SGP contribution of the quark-gluon correlation function with massless partons to the case of the three-gluon correlation functions with massive partons in the final state.

5.3 Contribution from $O(x, 0)$ and $N(x, 0)$

Next we consider the contribution from $O(x, 0)$ and $N(x, 0)$ in (23), which arise from the second terms in (24). For this purpose, we introduce the two fixed vectors $X^\mu = (0, 1, 0, 0)$ and $Y^\mu = (0, 0, 1, 0)$, and write

$$g_\perp^{\beta\gamma} = -X^\beta X^\gamma - Y^\beta Y^\gamma. \tag{31}$$

Then the derivative d/dp_c^γ hitting the FSI hard part in (23) for $O(x, 0)$ and $N(x, 0)$ can be written as

$$\frac{d}{dp_c^\gamma} H_{\alpha\beta}^{(F,j)}(xp, x'p', p_c) \delta\left(\tilde{s} + \tilde{t} + \tilde{u}\right) \left(g_\perp^{\beta\gamma} \epsilon^{\alpha p n S_\perp} + g_\perp^{\alpha\gamma} \epsilon^{\beta p n S_\perp} \right)$$

$$= -X^\mu \frac{d}{dp_c^\mu} H_{\alpha\beta}^{(F,j)}(xp, x'p', p_c) \delta\left(\tilde{s} + \tilde{t} + \tilde{u}\right) \left(X^\beta \epsilon^{\alpha p n S_\perp} + X^\alpha \epsilon^{\beta p n S_\perp} \right)$$

$$- Y^\mu \frac{d}{dp_c^\mu} H_{\alpha\beta}^{(F,j)}(xp, x'p', p_c) \delta\left(\tilde{s} + \tilde{t} + \tilde{u}\right) \left(Y^\beta \epsilon^{\alpha p n S_\perp} + Y^\alpha \epsilon^{\beta p n S_\perp} \right). \tag{32}$$

To perform the derivatives in this equation, we introduce the scalar functions $J_{1,2}^{(F,j)}(\tilde{s}, \tilde{t}, \tilde{u})$ $(j = d, f)$ by the decomposition:

$$H_{\alpha\beta}^{(F,j)}(xp, x'p', p_c) \left(X^\beta \epsilon^{\alpha p n S_\perp} + X^\alpha \epsilon^{\beta p n S_\perp} \right)$$

$$\equiv J_1^{(F,j)}(\tilde{s}, \tilde{t}, \tilde{u}, m_c^2) \left(p_c \cdot X \right) \epsilon^{p_c p n S_\perp} + J_2^{(F,j)}(\tilde{s}, \tilde{t}, \tilde{u}, m_c^2) \epsilon^{X p n S_\perp}, \tag{33}$$

14

where we used the kinematic condition $p_\perp^\gamma = p_\perp'^\gamma = 0$. One also obtains the similar decomposition for $H_{\alpha\beta}^{(F,j)}(xp, x'p', p_c)\left(Y^\beta \epsilon^{\alpha pnS_\perp} + Y^\alpha \epsilon^{\beta pnS_\perp}\right)$ by the replacement $X \to Y$ in (33) with the same functions $J_{1,2}^{(F,j)}$. Then the derivative in (32) can be performed with the help of (26) as

$$
-X^\mu \frac{d}{dp_c^\mu}\left[J_1^{(F,j)}(\tilde{s}, \tilde{t}, \tilde{u}, m_c^2)(p_c \cdot X)\epsilon^{p_c pnS_\perp}\delta\left(\tilde{s} + \tilde{t} + \tilde{u}\right)\right] + (X \to Y)
$$

$$
= 3\epsilon^{p_c pnS_\perp} J_1^{(F,j)}(\tilde{s}, \tilde{t}, \tilde{u}, m_c^2)\delta\left(\tilde{s} + \tilde{t} + \tilde{u}\right)
$$

$$
+ 2\vec{p}_{c\perp}^2 \epsilon^{p_c pnS_\perp}\left(\frac{\tilde{s}}{\tilde{t}}\right)\frac{\partial}{\partial\tilde{u}}\left(J_1^{(F,j)}(\tilde{s}, \tilde{t}, \tilde{u}, m_c^2)\delta\left(\tilde{s} + \tilde{t} + \tilde{u}\right)\right), \tag{34}
$$

$$
-X^\mu \frac{d}{dp_c^\mu}\left[J_2^{(F,j)}(\tilde{s}, \tilde{t}, \tilde{u}, m_c^2)\epsilon^{XpnS_\perp}\delta\left(\tilde{s} + \tilde{t} + \tilde{u}\right)\right] + (X \to Y)
$$

$$
= -2\epsilon^{p_c pnS_\perp}\frac{\tilde{s}}{\tilde{t}}\frac{\partial}{\partial\tilde{u}}\left(J_2^{(F,j)}(\tilde{s}, \tilde{t}, \tilde{u}, m_c^2)\delta\left(\tilde{s} + \tilde{t} + \tilde{u}\right)\right). \tag{35}
$$

Using these results and the relation $\vec{p}_{c\perp}^2 = \frac{\tilde{t}\tilde{u}}{\tilde{s}} - m_c^2$ in (32), and following the same procedure leading to (28), one obtains the FSI contribution with $O(x,0)$ and $N(x,0)$ in (23) in terms of $J_{1,2}^{(F,j)}$ in (33) as

$$
\int \frac{dx}{x^2}\frac{d}{dp_c^\gamma}H_{\alpha\beta}^{(F,d)}(xp, x'p', p_c)\delta\left(\tilde{s} + \tilde{t} + \tilde{u}\right)\left(g_\perp^{\beta\gamma}\epsilon^{\alpha pnS_\perp} + g_\perp^{\alpha\gamma}\epsilon^{\beta pnS_\perp}\right)O(x,0)
$$

$$
+ \left(H_{\alpha\beta}^{(F,d)} \to H_{\alpha\beta}^{(F,f)}, \ O(x,0) \to -N(x,0)\right)
$$

$$
= \epsilon^{p_c pnS_\perp}\int \frac{dx}{x^2}\left[3J_1^{(F,d)}O(x,0) + \frac{2\tilde{s}}{\tilde{t}\tilde{u}}\left(\frac{\tilde{t}\tilde{u}}{\tilde{s}} - m_c^2\right)\right.
$$

$$
\times \left\{\left(-J_1^{(F,d)} - m_c^2\frac{\partial J_1^{(F,d)}}{\partial m_c^2}\right)O(x,0) + J_1^{(F,d)}\left(x\frac{dO(x,0)}{dx} - 2O(x,0)\right)\right\}
$$

$$
- \frac{2\tilde{s}}{\tilde{t}\tilde{u}}\left\{-m_c^2\frac{\partial J_2^{(F,d)}}{\partial m_c^2}O(x,0) + J_2^{(F,d)}\left(x\frac{dO(x,0)}{dx} - 2O(x,0)\right)\right\}\left.\right]\delta\left(\tilde{s} + \tilde{t} + \tilde{u}\right)
$$

$$
+ \left(J_{1,2}^{(F,d)} \to J_{1,2}^{(F,f)}, \ O(x,0) \to -N(x,0)\right). \tag{36}
$$

The ISI contribution in (23) with $O(x,0)$ and $N(x,0)$ can also be obtained following the same procedure as above. Similarly to (33), one can decompose the ISI hard part as

$$
H_{\alpha\beta}^{(I,j)}(xp, x'p', p_c)\left(X^\beta \epsilon^{\alpha pnS_\perp} + X^\alpha \epsilon^{\beta pnS_\perp}\right)
$$

15

$$\equiv J_1^{(I,j)}(\tilde{s},\tilde{t},\tilde{u},m_c^2)\,(p_c \cdot X)\,\epsilon^{p_c p n S_\perp} + J_2^{(I,j)}(\tilde{s},\tilde{t},\tilde{u},m_c^2)\epsilon^{X p n S_\perp}$$

$$+ J_3^{(I,j)}(\tilde{s},\tilde{t},\tilde{u},m_c^2)\,(x'p' \cdot X)\,\epsilon^{p_c p n S_\perp} + J_4^{(I,j)}(\tilde{s},\tilde{t},\tilde{u},m_c^2)\,(p_c \cdot X)\,x'\epsilon^{p' p n S_\perp} \tag{37}$$

for $j = d, f$, where we ignored the terms which vanish in the limit $p'^\gamma_\perp \to 0$ after taking the derivative $d/d(x'p'^\gamma)$. Similar relation can be written down for $H_{\alpha\beta}^{(I,j)}(xp, x'p', p_c)\left(Y^\beta \epsilon^{\alpha p n S_\perp} + Y^\alpha \epsilon^{\beta p n S_\perp}\right)$, using the same functions $J_{1,2,3,4}^{(I,j)}$. Compared with (33), note the existence of the $J_{3,4}^{(I,j)}$ terms in (37), since one has to take the derivative with respect to $p'^\gamma_\perp$ before taking the $p'^\gamma_\perp \to 0$ limit. With these $J_{1,2,3,4}^{(I,j)}$, one eventually obtains the ISI contribution in (23) with $O(x,0)$ and $N(x,0)$ as

$$-\int \frac{dx}{x^2}\frac{d}{d(x'p'^\gamma)}H_{\alpha\beta}^{(I,d)}(xp, x'p', p_c)\delta\left(\tilde{s}+\tilde{t}+\tilde{u}\right)\left(g_\perp^{\beta\gamma}\epsilon^{\alpha p n S_\perp} + g_\perp^{\alpha\gamma}\epsilon^{\beta p n S_\perp}\right)O(x,0)$$

$$+ \left(H_{\alpha\beta}^{(I,d)} \to H_{\alpha\beta}^{(I,f)}, \ O(x,0) \to -N(x,0)\right)$$

$$= \epsilon^{p_c p n S_\perp}\int \frac{dx}{x^2}\left[\frac{2}{\tilde{u}}\left(\frac{\tilde{t}\tilde{u}}{\tilde{s}} - m_c^2\right)\left\{\left(J_1^{(I,d)} + m_c^2\frac{\partial J_1^{(I,d)}}{\partial m_c^2}\right)O(x,0)\right.\right.$$

$$\left. - J_1^{(I,d)}\left(x\frac{dO(x,0)}{dx} - 2O(x,0)\right)\right\}$$

$$+ \frac{2}{\tilde{u}}\left\{-m_c^2\frac{\partial J_2^{(I,d)}}{\partial m_c^2}O(x,0) + J_2^{(I,d)}\left(x\frac{dO(x,0)}{dx} - 2O(x,0)\right)\right\}$$

$$\left. - (2J_3^{(I,d)} + J_4^{(I,d)})O(x,0)\right]\delta\left(\tilde{s}+\tilde{t}+\tilde{u}\right)$$

$$+ \left(J_{1,2,3,4}^{(I,d)} \to J_{1,2,3,4}^{(I,f)}, \ O(x,0) \to -N(x,0)\right). \tag{38}$$

5.4 Twist-3 cross section from the $gg \to c\bar{c}$ scattering

Using the results (28), (30), (36) and (38) in (23), one obtains the final result for the total twist-3 single-spin-dependent cross section for $p^\uparrow p \to DX$ induced by the three-gluon correlation functions as

$$P_h^0\frac{d\Delta\sigma}{d^3 P_h} = \frac{2\pi M_N \alpha_s^2}{S}\epsilon^{P_h p n S_\perp}\int \frac{dx'}{x'}G(x')\int \frac{dz}{z^3}D_c(z)\int \frac{dx}{x^2}$$

$$\times\left[\left(\frac{2\tilde{s}}{\tilde{t}\tilde{u}}\right)\left\{m_c^2\frac{\partial K^{(F,d)}}{\partial m_c^2}O(x,x) - K^{(F,d)}\left(x\frac{dO(x,x)}{dx} - 2O(x,x)\right)\right\}\right.$$

$$+ \frac{2}{\tilde{u}}\left\{-m_c^2\frac{\partial K^{(I,d)}}{\partial m_c^2}O(x,x) + K^{(I,d)}\left(x\frac{dO(x,x)}{dx} - 2O(x,x)\right)\right\}$$

16

$$+ \left(O(x,x) \to N(x,x), \quad K^{(F,d)} \to K^{(F,f)}, \quad K^{(I,d)} \to K^{(I,f)} \right)$$

$$+ 3 J_1^{(F,d)} O(x,0) + \frac{2\tilde{s}}{\tilde{t}\tilde{u}} \left(\frac{\tilde{t}\tilde{u}}{\tilde{s}} - m_c^2 \right)$$

$$\times \left\{ \left(-J_1^{(F,d)} - m_c^2 \frac{\partial J_1^{(F,d)}}{\partial m_c^2} \right) O(x,0) + J_1^{(F,d)} \left(x \frac{dO(x,0)}{dx} - 2O(x,0) \right) \right\}$$

$$- \frac{2\tilde{s}}{\tilde{t}\tilde{u}} \left\{ -m_c^2 \frac{\partial J_2^{(F,d)}}{\partial m_c^2} O(x,0) + J_2^{(F,d)} \left(x \frac{dO(x,0)}{dx} - 2O(x,0) \right) \right\}$$

$$+ \left(O(x,0) \to -N(x,0), \quad J_{1,2}^{(F,d)} \to J_{1,2}^{(F,f)} \right)$$

$$+ \frac{2}{\tilde{u}} \left(\frac{\tilde{t}\tilde{u}}{\tilde{s}} - m_c^2 \right) \left\{ \left(J_1^{(I,d)} + m_c^2 \frac{\partial J_1^{(I,d)}}{\partial m_c^2} \right) O(x,0) - J_1^{(I,d)} \left(x \frac{dO(x,0)}{dx} - 2O(x,0) \right) \right\}$$

$$+ \frac{2}{\tilde{u}} \left\{ -m_c^2 \frac{\partial J_2^{(I,d)}}{\partial m_c^2} O(x,0) + J_2^{(I,d)} \left(x \frac{dO(x,0)}{dx} - 2O(x,0) \right) \right\} - (2J_3^{(I,d)} + J_4^{(I,d)}) O(x,0)$$

$$+ \left(O(x,0) \to -N(x,0), \quad J_{1,2,3,4}^{(I,d)} \to J_{1,2,3,4}^{(I,f)} \right) \Big] \delta \left(\tilde{s} + \tilde{t} + \tilde{u} \right). \tag{39}$$

where $K^{(B,j)}(\tilde{s}, \tilde{t}, \tilde{u}, m_c^2)$ $(B = F, I, j = d, f)$, $J_{1,2}^{(F,j)}(\tilde{s}, \tilde{t}, \tilde{u}, m_c^2)$ $(j = d, f)$ and $J_{1,2,3,4}^{(I,j)}(\tilde{s}, \tilde{t}, \tilde{u}, m_c^2)$ $(j = d, f)$ are the functions defined, respectively, in (25), (33) and (37) and can be calculated from the twist-2 diagrams in Fig. 2. By the direct calculation of these functions, we found that $J_1^{(F,j)}$ and $J_{1,3,4}^{(I,j)}$ $(j = d, f)$ are of $O(m_c^2)$ and thus vanish in the $m_c \to 0$ limit, and that $K^{(B,j)} = J_2^{(B,j)}$ $(B = F, I, j = d, f)$ at $m_c = 0$, which is consistent with the result in (15). For the twist-3 cross section for the $\bar{D}$-meson production, the sign of the contribution from $O(x,x)$ and $O(x,0)$ should be reversed in (39). The result calculated from (39), of course, agrees with (15) which were obtained by the direct calculation of Fig. 4.

The origin of the above master formula (39) is the relations in (19) and (20). Although they were derived in the LO QCD, the derivation was based on the quite general structure of the diagrams for the SGP contribution at $x_1 = x_2$ shown in Fig. 3, i.e., the coherent-gluon line is attached to the external parton line of the twist-2 diagrams in Fig. 1. As long as this structure is kept after including higher-order corrections, the relations (19) and (20) hold. Therefore we expect that the formula (39) will become a powerful tool to include high-order corrections to the twist-3 SSA [6].

6   Numerical calculation of the asymmetry

As is shown in (15), four nonperturbative functions $O(x, x)$, $N(x, x)$, $O(x, 0)$ and $N(x, 0)$ participate in the twist-3 cross section for A_N^D. Unlike twist-2 parton distributions, twist-3 multiparton correlation functions do not have probability interpretation and thus cannot be constrained by a certain positivity bound. [3] They have to be determined by comparing the calculated SSAs with experimental data, or by some nonperturbative techniques in QCD. At present there is no information on these functions. Preliminary data on A_N^D by the PHENIX collaboration [26] suggests $|A_N^D| \leq 5$ % in the region $|x_F| < 0.1$ at $\sqrt{S} = 200$ GeV. Since the unpolarized cross section for the pion production at RHIC has been well described by the next-to-leading order (NLO) calculation in the collinear factorization [30, 31, 32], comparison of the asymmetry calculated by our twist-3 cross section with the RHIC data will be the first step for determining the magnitude of the three-gluon correlation functions in the nucleon. [4] Here we present a simple model calculation of the asymmetry at the RHIC energy taking into account of the preliminary RHIC data.
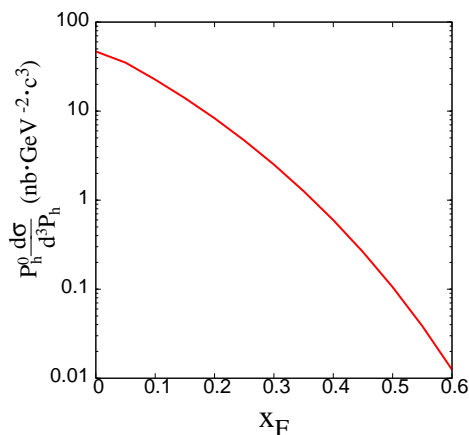

Figure 5: Unpolarized cross section for $pp \to DX$ by the gluon fusion process at the RHIC energy $\sqrt{S} = 200$ GeV and $P_T = 2$ GeV.

To see the relative importance of each term appearing in (15), we assume the same form for the four nonperturbative functions as [5]

$$O(x, x) = O(x, 0) = N(x, x) = -N(x, 0). \tag{40}$$

As a functional form of these functions, we employ the following ansatz:

$$\text{Model 1}: \quad O(x, x) = K_G \, x \, G(x), \tag{41}$$

---

[3]For a comprehensive review on the positivity bounds of parton distributions, see [29].

[4]The size of the NLO correction to the twist-3 cross section in (15) could be different from that for the twist-2 unpolarized cross section, which may lead to significantly different A_N^D. One thus should take the present calculation as only an estimate of the order-of-magnitude.

[5]Minus sign is introduced for $N(x, 0)$, since $\hat{\sigma}^{N2}$ has an opposite sign compared with $\hat{\sigma}^{O1, O2, N1}$.

$$\text{Model 2:} \qquad O(x,x) = K_G' \sqrt{x}\, G(x), \tag{42}$$

where $G(x)$ is the twist-2 unpolarized gluon density, and K_G and K_G' are the constants which we determine so that the calculated asymmetry is consistent with the RHIC data. Since the

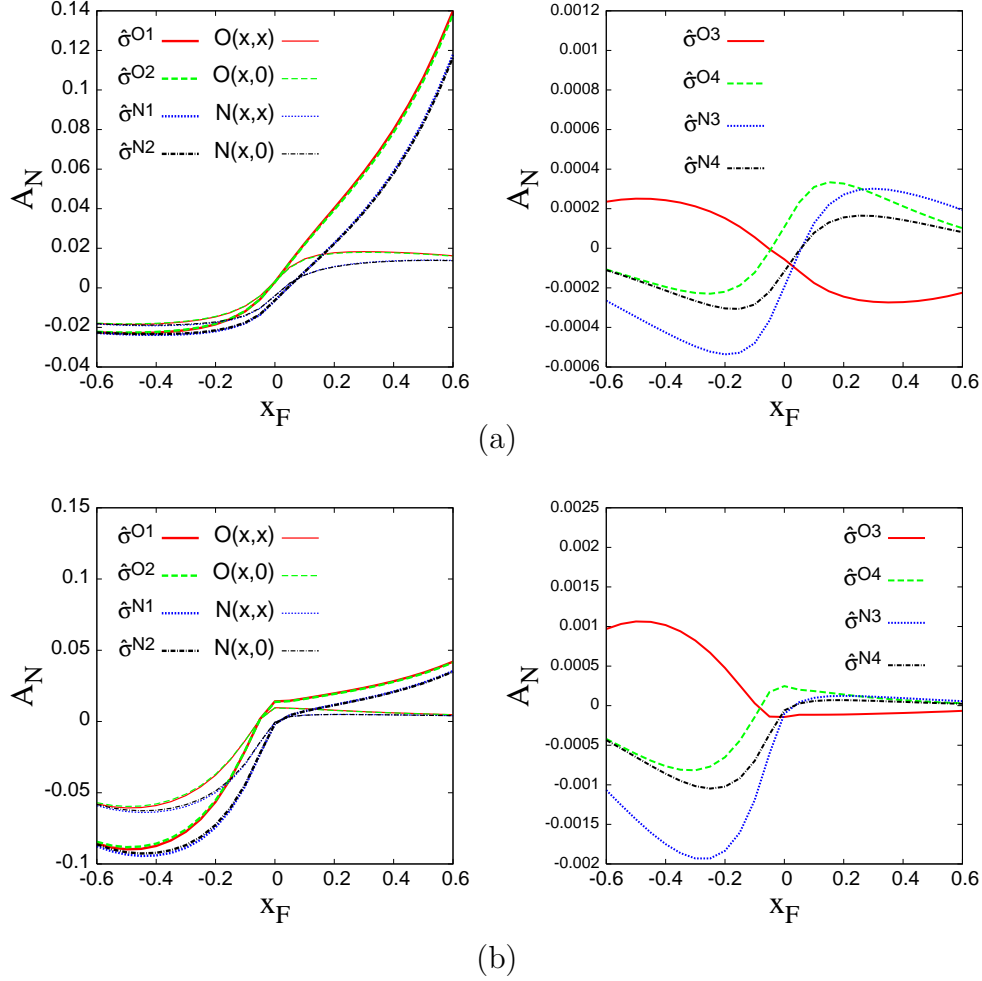Figure 6: (a) Contribution to A_N^D from the 8 components proportional to $\sigma^{O1,O2,N1,N2}$ (left) and $\sigma^{O3,O4,N3,N4}$ (right) in (15) obtained by using the model 1 in (41) with $K_G = 0.002$. In the left figure, the non-derivative terms contributing with $\sigma^{O1,O2,N1,N2}$ are also plotted by thin lines labeled by $O(x,x)$, $O(x,0)$, $N(x,x)$ and $N(x,0)$. (b) The same as (a) but for the model 2 in (42) with $K_G' = 0.0005$.

three-gluon correlation functions are completely independent from the gluon density, the above parametrization is a very crude approximation and the result below should be taken only as an estimate of the order-of-magnitude for the three-gluon correlation functions. But they are useful to get the shape and magnitude of the three-gluon correlation functions relative to the gluon density. Note that the above two models monitor the sensitivity of A_N^D

to the small-x behavior of the three-gluon correlation functions. For the numerical calculation, we use GJR08 distribution [33] for $G(x)$ and KKKS08 fragmentation function [34] for $D_f(z)$. We also assume the same scale dependence for $O(x, x)$ *etc* as $G(x)$ for simplicity. We calculate A_N for the D and $\bar{D}$ mesons at the RHIC energy of $\sqrt{S} = 200$ GeV and the transverse momentum of the D-meson $P_T = 2$ GeV with the parameter $m_c = 1.3$ GeV by setting the scale of all the distribution and fragmentation functions at $\mu = \sqrt{P_T^2 + m_c^2}$.

For completeness, we first show in Fig. 5 the unpolarized cross section for $pp \to DX$ based on the gluon fusion process (6) at $\sqrt{S} = 200$ GeV and $P_T = 2$ GeV. This will constitute the denominator of A_N^D in our calculation below.
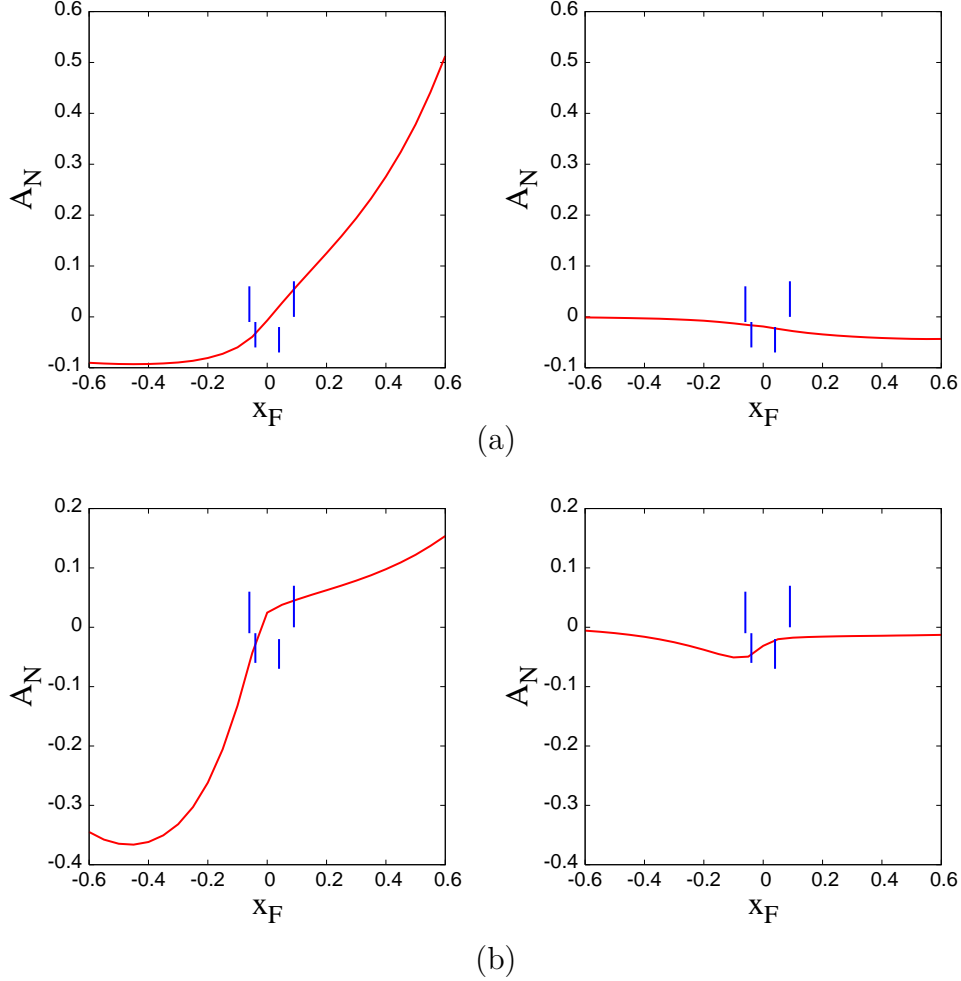

(a)

(b)

Figure 7: (a) A_N^D for the D^0 (left) and $\bar{D}^0$ (right) mesons for Model 1 in (41) with $K_G = 0.002$. (b) A_N^D for the D^0 (left) and $\bar{D}^0$ (right) mesons for Model 2 in (42) with $K_G' = 0.0005$. Bars denote the RHIC preliminary data taken from [26].

Fig. 6 shows the results for the contribution to A_N^D from each term in the twist-3 cross section shown in (15) with $K_G = 0.002$ for the model 1 (Fig. 6(a)) and $K_G' = 0.0005$ for

the model 2 (Fig. 6(b)). For both models, one sees that the nonderivative terms accompanying the hard cross sections $\hat{\sigma}^{O3,O4,N3,N4}$ is negligible compared to the contributions from $\hat{\sigma}^{O1,O2,N1,N2}$. In the left figures of Figs. 6 (a) and (b), we have also plotted the contribution from the nonderivative terms proportional to $\hat{\sigma}^{O1,O2,N1,N2}$, which shows that the derivative contributions dominate in these terms at large x_F (> 0), while the effect of the nonderivative term becomes important at $x_F < 0$ and even dominates the asymmetry for the model 1. One also sees that $\hat{\sigma}^{O1}$ and $\hat{\sigma}^{O2}$ give rise to numerically very close asymmetries at the RHIC energy for the two models, and likewise for $\hat{\sigma}^{N1}$ and $\hat{\sigma}^{N2}$. The asymmetries caused by $\hat{\sigma}^{O1,O2}$ and $\hat{\sigma}^{N1,N2}$ are also similar.

Fig. 7 shows the result for A_N^D for the D and $\bar{D}$ mesons including all the contributions in (15) together with the preliminary data by the PHENIX collaboration [26]. Because the sign of the contribution from $\{O(x,x), O(x,0)\}$ changes between D and $\bar{D}$ as shown in (15), $\{O(x,x), O(x,0)\}$ and $\{N(x,x), N(x,0)\}$ contribute to the asymmetry constructively (destructively) for the D ($\bar{D}$) meson, leading to a large (small) A_N^D for D ($\bar{D}$). If one reverses the relative sign between O and N from (40), the result for the D and $\bar{D}$ mesons will be interchanged. The values $K_G = 0.002$ and $K_G' = 0.0005$ have been chosen such that the calculated asymmetries does not overshoot the data for A_N for the D-meson (left figures in Figs. 7(a) and (b)) under the assumption (40). By comparing the results for the models 1 and 2 in Fig. 7, one sees that the behavior of the asymmetry at $x_F < 0$ depends strongly on the small-x behavior of the three gluon correlation functions. Therefore A_N^D at $x_F < 0$ is useful to get constraint on the small-x behavior of the three-gluon correlation functions.

As we saw in the left figures of Fig. 6, we found the relations $\hat{\sigma}^{O1} \simeq \hat{\sigma}^{O2}$ and $\hat{\sigma}^{N1} \simeq \hat{\sigma}^{N2}$. This means that the combinations $O(x,x) + O(x,0)$ and $N(x,x) - N(x,0)$ can be taken as good effective three-gluon correlation functions determining A_N^D's at RHIC energies. From the left figures in Figs. 7 (a) and (b), if the ansatz (41) or (42) is a reasonable assumption for the x-dependence of the three-gluon correlation functions, $K_G = 0.002$ or $K_G' = 0.0005$ can be taken as a modest upper bound corresponding to the assumptions (41) and (42). Therefore we may set the upper bound for the combination as

$$|O(x,x) + O(x,0)| \leq 0.004\, x\, G(x), \qquad |N(x,x) - N(x,0)| \leq 0.004\, x\, G(x), \qquad (43)$$

and

$$|O(x,x) + O(x,0)| \leq 0.001\sqrt{x}\, G(x), \qquad |N(x,x) - N(x,0)| \leq 0.001\sqrt{x}\, G(x), \qquad (44)$$

although extraction of the separate constraint on the four functions is not possible. [6] We remark that even though the RHIC data suggests small A_N^D at $|x_F| < 0.1$, it can be much larger at $|x_F| > 0.1$ depending on the behavior of the three-gluon correlation functions in the large and small x regions as shown in Fig. 7.

---

[6]In [5], we extracted a stronger constraint for the upper bound of $|O(x,x) + O(x,0)|$ and $|N(x,x) - N(x,0)|$, since we assumed $|A_N^D| < 5$ % in the wider region of x_F, while the data showing $|A_N^D| < 5$ % is only in the region $|x_F| < 0.1$ [26]. Therefore, at present, a weaker upper bound in (43) and (44) is more appropriate.

7 Summary

In this paper we have studied the SSA for the open-charm production in the pp collision, $p^\uparrow p \to DX$, based on the twist-3 mechanism in the collinear factorization. Since the three-gluon correlation functions in the transversely polarized nucleon play a dominant role in giving rise to SSA for this process, we have derived the corresponding twist-3 single-spin-dependent cross section in the leading order QCD. As in the case of our previous study on $ep^\uparrow \to eDX$, our result differs from the existing result in the literature. We have also derived the master formula which shows that the corresponding twist-3 cross section can be obtained from the hard part for the $gg \to c\bar{c}$ scattering in the twist-2 level. The use of this formula simplifies the actual calculation and is useful to make the structure of the twist-3 cross section transparent. We expect that this master formula is useful for the inclusion of the higher-order corrections to the cross section. We also presented a model calculation of the asymmetry A_N^D in comparison to the preliminary data obtained at RHIC. We have shown that A_N^D at $x_F < 0$ is sensitive to the small-x behavior of the three-gluon correlation functions, and have given a modest upper limit on those functions.

Acknowledgments

A Ward identity for the initial state interaction

To derive the cross section for $p^\uparrow p \to DX$, one has to analyze

$$\int \frac{d^4k_1}{(2\pi)^4} \int \frac{d^4k_2}{(2\pi)^4}\, S_{\mu\nu\lambda}^{abc}(k_1, k_2, x'p', p_c) M_{abc}^{\mu\nu\lambda}(k_1, k_2), \tag{45}$$

where $M_{abc}^{\mu\nu\lambda}(k_1, k_2)$ is defined in (11) and $S_{\mu\nu\lambda}^{abc}(k_1, k_2, x'p', p_c)$ is the corresponding hard part as shown in Fig. 3. As was shown in [4], in order to be able to obtain the cross section from (13), it is essential that $S_{\mu\nu\lambda}^{abc}(k_1, k_2, x'p', p_c)$ satisfies the Ward identities

$$k_1^\mu S_{\mu\nu\lambda}^{abc}(k_1, k_2) = 0, \qquad k_2^\nu S_{\mu\nu\lambda}^{abc}(k_1, k_2) = 0, \qquad (k_2 - k_1)^\lambda S_{\mu\nu\lambda}^{abc}(k_1, k_2) = 0. \tag{46}$$

It is easy to see that the hard part for the sum of the FSI diagrams shown in Fig. 4(a) satisfies (46) due to the on-shell condition for the bared quark-lines. However, the hard part for the ISI diagrams in Fig. 4(b) does not satisfy (46). This is because the polarization tensor for the gluon line producing the SGP (bared gluon line in Fig. 4(b)) is taken to be $-g_{\sigma\tau}$ in the Feynman gauge, which contains the contribution from unphysical polarizations. Nevertheless, one can calculate the hard cross section for the ISI from (13). To show this,

we define the new hard part for the ISI, $\widetilde{S}_{\mu\nu\lambda}^{I,abc}(k_1, k_2, x'p', p_c)$, which is obtained from the original hard part for ISI, $S_{\mu\nu\lambda}^{I,abc}(k_1, k_2, x'p', p_c)$, by replacing the polarization tensor for the bared gluon-propagator in Fig. 4(b) as

$$-g_{\sigma\tau} \rightarrow -g_{\sigma\tau} + \frac{q_\sigma p_\tau + q_\tau p_\sigma}{q \cdot p}, \tag{47}$$

where q is the momentum carried by the bared gluon-line. One can show that in the twist-3 accuracy this $\widetilde{S}_{\mu\nu\lambda}^{I,abc}(k_1, k_2, x'p', p_c)$ satisfies the relation

$$\int \frac{d^4 k_1}{(2\pi)^4} \int \frac{d^4 k_2}{(2\pi)^4} S_{\mu\nu\lambda}^{I,abc}(k_1, k_2, x'p', p_c) M_{abc}^{\mu\nu\lambda}(k_1, k_2)$$

$$= \int \frac{d^4 k_1}{(2\pi)^4} \int \frac{d^4 k_2}{(2\pi)^4} \widetilde{S}_{\mu\nu\lambda}^{I,abc}(k_1, k_2, x'p', p_c) M_{abc}^{\mu\nu\lambda}(k_1, k_2), \tag{48}$$

where $M_{abc}^{\mu\nu\lambda}(k_1, k_2)$ is defined in (11). The extra terms in $\widetilde{S}_{\mu\nu\lambda}^{I,abc}(k_1, k_2, x'p', p_c)$ compared to $S_{\mu\nu\lambda}^{I,abc}(k_1, k_2, x'p', p_c)$ which occur due to the replacement (47) can be shown to vanish with the help of the Feynman gauge condition for the matrix element:

$$k_{1\mu} M_{abc}^{\mu\nu\lambda}(k_1, k_2) = 0, \quad k_{2\nu} M_{abc}^{\mu\nu\lambda}(k_1, k_2) = 0, \quad (k_2 - k_1)_\lambda M_{abc}^{\mu\nu\lambda}(k_1, k_2) = 0. \tag{49}$$

From the above relation, one can use $\widetilde{S}_{\mu\nu\lambda}^{I,abc}(k_1, k_2, x'p', p_c)$ for the calculation of the twist-3 cross section. Since $\widetilde{S}_{\mu\nu\lambda}^{I,abc}(k_1, k_2)$ satisfies

$$k_1^\mu \widetilde{S}_{\mu\nu\lambda}^{I,abc}(k_1, k_2) = 0, \quad k_2^\nu \widetilde{S}_{\mu\nu\lambda}^{I,abc}(k_1, k_2) = 0, \quad (k_2 - k_1)^\lambda \widetilde{S}_{\mu\nu\lambda}^{I,abc}(k_1, k_2) = 0, \tag{50}$$

the resulting twist-3 cross section from the ISI takes the form of (13) with $S_{\mu\nu\lambda}^{abc}(k_1, k_2, x'p', p_c)$ replaced by $\widetilde{S}_{\mu\nu\lambda}^{I,abc}(k_1, k_2, x'p', p_c)$. Finally, one can show the relation

$$\left. \frac{\partial \widetilde{S}_{\mu\nu\lambda}^{I,abc}(k_1, k_2, x'p', p_c) p^\lambda}{\partial k_2^\sigma} \right|_{k_i = x_i p} \omega^\mu{}_\alpha \omega^\nu{}_\beta \omega^\sigma{}_\gamma M_{F,abc}^{\alpha\beta\gamma}(x_1, x_2)$$

$$= \left. \frac{\partial S_{\mu\nu\lambda}^{I,abc}(k_1, k_2, x'p', p_c) p^\lambda}{\partial k_2^\sigma} \right|_{k_i = x_i p} \omega^\mu{}_\alpha \omega^\nu{}_\beta \omega^\sigma{}_\gamma M_{F,abc}^{\alpha\beta\gamma}(x_1, x_2), \tag{51}$$

where the right-hand-side is calculated with the original hard part for the ISI. This way one can obtain the contribution of the three-gluon correlation functions to the twist-3 cross section from (13).

References

[1] X. Ji, Phys. Lett. **B289**, 137 (1992).

[2] Z. B. Kang and J. W. Qiu, Phys. Rev. D **78** (2008) 034005.

[3] Z. B. Kang, J. W. Qiu, W. Vogelsang and F. Yuan, Phys. Rev. **D78**, 114013 (2008).

[4] H. Beppu, Y. Koike, K. Tanaka and S. Yoshida, Phys. Rev. D **82**, 054005 (2010).

[5] Y. Koike and S. Yoshida, in the proceedings of 19th International Spin Physics Symposium (SPIN2010), Julich, Germany, Sep. 27-Oct. 2, 2010. arXiv:1012.1064 [hep-ph].

[6] Y. Koike, K. Tanaka and S. Yoshida, arXiv:1104.0798 [hep-ph].

[7] A. V. Efremov and O. V. Teryaev, Sov. J. Nucl. Phys. **36** (1982) 140 [Yad. Phiz. **36** (1982) 242]; Phys. Lett. **B150** (1985) 383.

[8] J. Qiu and G. Sterman, Nucl. Phys. **B378** (1992) 52; Phys. Rev. **D59** (1998) 014004.

[9] H. Eguchi, Y. Koike and K. Tanaka, Nucl. Phys. **B763** (2007) 198.

[10] Y. Kanazawa and Y. Koike, Phys. Lett. **B478** (2000) 121; Phys. Lett. **B490** (2000) 99; Phys. Rev. **D64** 034019 (2001).

[11] H. Eguchi, Y. Koike and K. Tanaka, Nucl. Phys. **B752** (2006) 1.

[12] X. D. Ji, J. W. Qiu, W. Vogelsang and F. Yuan, Phys. Rev. Lett. **97** (2006) 082002; Phys. Rev. **D73** (2006) 094017.

[13] X. D. Ji, J. W. Qiu, W. Vogelsang and F. Yuan, Phys. Lett. **B638** (2006) 178.

[14] Y. Koike, W. Vogelsang and F. Yuan, Phys. Lett. B **659** (2008) 878.

[15] C. Kouvaris, J. W. Qiu, W. Vogelsang and F. Yuan, Phys. Rev. D **74** (2006) 114013.

[16] Y. Koike and K. Tanaka, Phys. Lett. B **646** (2007) 232 [Erratum-ibid. B **668** (2008) 458]

[17] Y. Koike and K. Tanaka, Phys. Rev. D **76** (2007) 011502

[18] F. Yuan and J. Zhou, Phys. Lett. B **668** (2008) 216.

[19] J. Zhou, F. Yuan and Z. T. Liang, Phys. Rev. D **78**, 114008 (2008).

[20] Y. Koike and T. Tomita, Phys. Lett. **B675** (2009) 181.

[21] K. Kanazawa and Y. Koike, Phys. Rev. D **82**, 034009 (2010).

[22] A. Metz and J. Zhou, arXiv:1006.3097 [hep-ph].

[23] K. Kanazawa and Y. Koike, arXiv:1104.0117 [hep-ph].

[24] P. J. Mulders and J. Rodrigues, Phys. Rev. **D63**, 094021 (2001).

[25] M. Anselmino, M. Boglione, U. D'Alesio, E. Leader and F. Murgia, Phys. Rev. D **70**, 074025 (2004).

[26] H. Liu [PHENIX Collaboration], AIP Conf. Proc. **1149** (2009) 439.

[27] A. V. Belitsky, X. D. Ji, W. Lu, J. Osborne, Phys. Rev. **D63**, 094012 (2001).

[28] V.M. Braun, A.N. Manashov, B. Pirnay, Phys. Rev. **D80**, 114002 (2009).

[29] X. Artru, M. Elchikh, J.M. Richard, J. Soffer, O.V. Teryaev, Phys. Rep. **470** 1, (2009).

[30] B. Jäger, A. Schäfer, M. Stratmann, and W. Vogelsang, Phys. Rev. D **67**, 054005 (2003).

[31] STAR Collaboration, J. Adams *et al.*, Phys. Rev. Lett. **92**, 171801 (2004).

[32] PHENIX Collaboration, S. S. Adler *et al.*, Phys. Rev. Lett. **95**, 202001 (2005).

[33] M. Gluck, P. Jimenez-Delgado, and E. Reya, Eur. Phys. J. **C53** 355 (2008).

[34] T. Kneesch, B.A. Kniehl, G. Kramer, and I. Schienbein, Nucl. Phys. **B799** 34 (2008).